The Behavior of a Simple Hurricane Model Using a Convective Scheme Based on Subcloud-Layer Entropy Equilibrium

KERRY A. EMANUEL

Center for Meteorology and Physical Oceanography, Massachusetts Institute of Technology, Cambridge, Massachusetts

(Manuscript received 11 August 1994, in final form 23 March 1995)

ABSTRACT

Recent work on the interaction of convection with large-scale flows suggests that a closure based on a presumed equilibrium between surface enthalpy fluxes and input of low-entropy air into the subcloud layer by convective downdrafts works well in models of the tropical atmosphere. Such a convective representation is here used in a simple numerical tropical cyclone model. This further simplifies the model, while in many respects improving its performance.

1. Introduction

Most convection in the Tropics originates from the comparatively thin subcloud layer, for it is this layer that receives direct heat input from the underlying surface. At the same time, the thermodynamic disequilibrium between the subcloud-layer air and the underlying ocean is large enough that, were they unopposed, surface fluxes would bring the subcloud entropy into equilibrium with the surface in about 12 hours. In nature, however, the surface enthalpy fluxes are very nearly balanced by the entrainment of low-entropy air through the top of the layer. In undisturbed conditions, this entrainment is accomplished by small-scale turbulence acting on a pronounced negative jump of entropy across the top of the layer, while in regimes experiencing deep convection, convective downdrafts are the principal agents for importing low-entropy air.

The near balance of the subcloud-layer entropy budget was used by Emanuel (1993) to determine the convective updraft mass flux out of the boundary layer in a simple model of intraseasonal oscillations in convecting atmospheres. Recently, Raymond (1995) has more thoroughly discussed the physical basis for such a representation of convection. The basic idea can be illustrated using the vertically averaged budget of entropy ($s_b = c_p \ln\theta_e$) in the subcloud layer:

$$h\frac{ds_b}{dt} = \frac{1}{T_b} C_D|\mathbf{V}_b|(k_s^* - k_b) + (M_d + w_e)(s_b - s_m) + h\frac{\dot{Q}_{\text{rad}}}{T_b}, \quad (1)$$

where h is the depth of the subcloud layer, T_b and $|\mathbf{V}_b|$ are the near-surface air temperature and wind speed, C_D is an exchange coefficient, k_b is the enthalpy of air near the sea surface $\{k = [c_{pd}(1 - q) + c_l q]T + L_v q$, where T and q are the temperature and specific humidity, c_{pd} and c_l are the heat capacity at constant pressure of dry air and the heat capacity of liquid water, respectively, and L_v is the latent heat of vaporization$\}$, k_s^* is the saturation enthalpy at sea surface temperature, M_d is the convective downdraft volume flux at cloud base, w_e is the vertical velocity outside of the clouds at the top of the subcloud layer (assumed negative here), s_m is the entropy of air above the subcloud layer, and $\dot{Q}_{\text{rad}}$ is the radiative cooling in the subcloud layer. It has been assumed that dry turbulence at the top of the subcloud layer and convective downdrafts both import the same value of entropy, s_m, into the subcloud layer; this has been done for simplicity but is not necessary for the following development.

The quasi-equilibrium assumption for the subcloud-layer entropy neglects the time tendency of entropy and the radiative cooling terms in comparison to the surface and downdraft fluxes, which are thus assumed to be in equilibrium, yielding

$$M_d + w_e \approx -\frac{C_D|\mathbf{V}_b|(k_s^* - k_b)}{T_b(s_b - s_m)}. \quad (2)$$

At the same time, mass continuity at the top of the subcloud layer demands that

$$M_d + w_e + M_u = w_+, \quad (3)$$

where M_u is the net convective updraft mass flux at cloud base, and w_+ is the total (large-scale) vertical velocity at cloud base. Combining (3) and (2) gives

$$M_u = w_+ + \frac{C_D|\mathbf{V}_b|(k_s^* - k_b)}{T_b(s_b - s_m)}, \quad (4)$$

Corresponding author address: Dr. Kerry A. Emanuel, Center for Meteorology and Physical Oceanography, Massachusetts Institute of Technology, Room 54-1620, Cambridge, MA 02139.

subject to $M_u \geq 0$. [This is nearly identical to (11) of Emanuel (1993).] Thus, the convective updraft mass flux is related to the mean ascent at the top of the subcloud layer and the surface enthalpy flux. In most tropical circulations, the contribution to M_u from w is somewhat larger than that from variable surface fluxes, but in waves such as the Madden–Julian oscillation (MJO), the phase of the surface flux term contributes to wave growth, while that from w alters the phase speed of the disturbances but does not amplify them.

Although (4) provides a diagnostic expression for the convective *updraft* mass flux at the top of the subcloud layer, the *net* convective mass flux, $M_u + M_d$, is needed to predict temperature changes in the free atmosphere, for it is this sum that forces compensating subsidence. We begin by writing the equation for potential temperature just above the top of the subcloud layer, θ_+:

$$\frac{d_h \ln\theta_+}{dt} = (M_u + M_d - w_+)\frac{\partial \ln\theta}{\partial z} + \frac{\dot{Q}_{\rm rad}}{c_p T_+}, \quad (5)$$

where

$$\frac{d_h}{dt} \equiv \frac{\partial}{\partial t} + \mathbf{V}_H \cdot \nabla,$$

$\mathbf{V}_H$ is the horizontal velocity vector, and T_+ is the temperature just above the subcloud layer.

It is clear from (5) that a relationship between the convective updraft and downdraft mass fluxes is needed. This must be provided, in general, by a cloud model. For the purposes of constructing a maximally simple model of the MJO, Yano and Emanuel (1991) and Emanuel (1993) related M_d to M_u just above cloud base by

$$M_d = -(1 - \epsilon_p)M_u, \quad (6)$$

where ϵ_p is a bulk precipitation efficiency, which is in general a function of cloud water distributions and environmental temperature and humidity. If all the rain evaporates, $\epsilon_p = 0$ and $M_d = -M_u$, consistent with the fact that there is then no net latent heat release. If, on the other hand, $\epsilon_p = 1$, $M_d = 0$: there is no evaporation to drive a downdraft.[1] In this model, ϵ_p will be specified as a function of environmental relative humidity only.

We now substitute (4) and (6) into (5) to obtain

$$\frac{d_h \ln\theta_+}{dt} = \left[\epsilon_p \frac{C_D|\mathbf{V}_b|(k_s^* - k_b)}{T_b(s_b - s_m)} - (1 - \epsilon_p)w_+\right] \times \frac{\partial \ln\theta}{\partial z} + \frac{\dot{Q}_{\rm rad}}{c_p T_+}. \quad (7)$$

This shows that actual temperature changes just above the top of the subcloud layer are driven by surface enthalpy fluxes, radiative cooling, and adiabatic cooling related to large-scale ascent. Note that the effective stratification is proportional to $1 - \epsilon_p$; Yano and Emanuel (1991) and Emanuel (1993) argue that this accounts for the small phase speed of the MJO, consistent with observations and with models using linearizations of the Betts–Miller cumulus parameterization (Neelin and Yu 1994; Emanuel et al. 1994).

Before proceeding, we express (7) in a slightly different form by using the saturation entropy, s^*, in place of θ. (The saturation entropy is the entropy the air would have were it saturated at the same pressure and temperature; it is a state variable and may also be expressed as $c_p \ln\theta_e^*$, where θ_e^* is the saturation equivalent potential temperature.) The relationship between fluctuations at constant pressure of s^* and $\ln\theta$ is (e.g., see Emanuel 1994a)

$$\delta_p s^* = c_p \frac{\Gamma_d}{\Gamma_m} \delta_p \ln\theta, \quad (8)$$

where c_p is a heat capacity at constant pressure and Γ_d and Γ_m are the dry and moist adiabatic lapse rates, respectively. Using (8), (7) may be written

$$\frac{d_h s_+^*}{dt} = c_p\left[\epsilon_p \frac{C_D|\mathbf{V}_b|(k_s^* - k_b)}{T_b(s_b - s_m)} - (1 - \epsilon_p)w_+\right] \times \frac{\Gamma_d}{\Gamma_m}\frac{\partial \ln\theta}{\partial z} + \frac{\Gamma_d}{\Gamma_m}\frac{\dot{Q}_{\rm rad}}{T_+}, \quad (9)$$

where s_+^* is the saturation entropy just above the subcloud layer.

We now argue that to a first approximation, s^* is constant through the depth of the convecting layer. To begin with, several arguments have been advanced (e.g., Bretherton and Smolarkiewicz 1989) that entrainment, and therefore mass flux, is related to the variation of cloud buoyancy with height. This supports the device, used in many convective schemes (e.g., Manabe et al. 1965; Betts 1986) of driving actual lapse rates toward moist adiabatic lapse rates. We shall assume here that the lapse rate in the convecting layer is maintained by convection at its moist adiabatic value. Neglecting the direct effect of water substance on density, this is equivalent to assuming that s^* is constant with height and equal to its value, s_+^*, just above the top of the subcloud layer. This assumption was also made by Emanuel (1993). Thus (9) may be regarded as a prediction equation for temperature throughout the depth of the convecting layer. In general, this depth must also be predicted or diagnosed; here we take it to have a fixed value for simplicity.

Up until now we have assumed that convection responds instantly to changes in the large-scale forcing. But even though it is small, the timescale of convection has been shown to have important effects in global

[1] Raymond (1995) uses an expression like (6) but with α replacing $1 - \epsilon_p$. We emphasize that (6) is a crude approximation; in a more complete treatment M_d must be related to M_u through a cloud model.

models (Betts and Miller 1986) and in idealized models of intraseasonal oscillations in the Tropics (Emanuel 1993; Neelin and Yu 1994). We account for this timescale here using the same approach as Emanuel (1993). We regard (4) as an expression for the *equilibrium* updraft mass flux, $M_{u_{eq}}$,

$$M_{u_{eq}} = w_+ + \frac{C_D|\mathbf{V}_b|(k_s^* - k_b)}{T_b(s_b - s_m)}, \qquad (10)$$

and relax the actual updraft mass flux to this value using

$$\frac{d_h M_u}{dt} = \frac{M_{u_{eq}} - M_u}{\tau_c}, \qquad (11)$$

with $M_{u_{eq}}$ given by (10) and τ_c taken to be on the order of a few hours. The saturation entropy through the depth of the convecting layer (which is assumed equal to s_+^*) is then predicted using (5), (6), and (8):

$$\frac{d_h s^*}{dt} = c_p(\epsilon_p M_u - w_+)\frac{\Gamma_d}{\Gamma_m}\frac{\partial \ln\theta}{\partial z} + \frac{\Gamma_d}{\Gamma_m}\frac{\dot{Q}_{\mathrm{rad}}}{T_+}. \qquad (12)$$

It should be understood that all the quantities on the right side of (12) are to be evaluated just above the top of the subcloud layer.

Finally, it is necessary to predict the distributions of subcloud-layer entropy, s_b, and the entropy at the source level for downdrafts, s_m, used in (10). [In the linearized version of (10) used by Yano and Emanuel (1991) and Emanuel (1993), fluctuations of s_b and s_m in (10) were ignored, so this was not necessary.] In regions where it exists, convection can be assumed to tie the subcloud-layer entropy to the value of s^* at the subcloud-layer top, so that the subcloud-layer air is approximately neutral to small upward displacements. In regions of strong large-scale descent, however, deep convection may cease, and in that case it is necessary to solve the subcloud-layer entropy equation (1). In general, the subcloud-layer entropy may always be determined by (1) subject to the constraint

$$s_b \leq s^*, \qquad (13)$$

where s^* is the saturation entropy above the subcloud layer.

We summarize this approach to representing deep convection as follows.

1) The equilibrium deep convective downdraft mass flux is determined by requiring equilibrium of the subcloud-layer entropy; this results in (2).

2) The equilibrium deep convective updraft mass flux is related to the equilibrium downdraft mass flux and the large-scale vertical velocity by mass continuity, resulting in (10).

3) The actual deep convective mass flux is relaxed to its equilibrium value over a finite timescale, τ_c, using (11).

4) The determination of the saturation entropy just above the top of the subcloud layer requires knowledge of the total convective mass flux (the sum of the updraft and downdraft mass fluxes); this in turn requires a relationship between M_u and M_d. The simplest approach relates the two linearly; this results in (12) for the saturation entropy, s_+^*, just above the subcloud layer.

5) To get the temperature (or equivalently, s^*) through the rest of the convecting layer, it is assumed that the layer temperature relaxes toward a moist adiabat (s^* constant with height) at some rate. Assumptions about the magnitude of this rate vary greatly. We follow Emanuel (1993) and assume that s^* is constant with height at all times, but relax the strict equilibrium of the boundary layer by introducing (11).

6) The entropy of the subcloud layer is obtained by assuming convective neutrality, $s_b = s^*$, except where large-scale conditions prohibit deep convection, in which case the subcloud-layer entropy budget must be explicitly calculated using (1). Both cases may be satisfied simply by solving (1) subject to the constraint (13).

7) A budget equation for the entropy, s_m, at the source level for convective downdrafts must be solved.

Note that point 1 is a *quasi*-equilibrium assumption on boundary-layer entropy, which does vary slowly and is predicted according to point 6. Other aspects of this way of representing moist convection are discussed in some detail in Raymond (1995).

When a version of this simple way of representing convection is used in a model of the equatorial beta plane, linearized about mean easterly flow, unstable modes representing slow, eastward-propagating planetary Kelvin waves and westward-propagating synoptic-scale waves with structures similar to mixed Rossby–gravity modes emerge. Emanuel (1993) also showed that in order to model these properly, the small time lags over which convection relaxes the tropospheric temperature to a moist adiabat are crucial; strict quasi-equilibrium of the Arakawa–Schubert (1974) kind results in spurious high-frequency modes.

The purpose of this paper is to show that the simple way of representing convection reviewed above also performs very well in a simple hurricane model.

2. Hurricane model[2]

Except for the convective parameterization and a few minor changes, the hurricane model used here is identical to that of Emanuel (1989, hereafter E89). We here summarize the properties of the model and the changes that have been made to E89; the actual model equations are presented in the appendix.

[2] The model described herein is available from the author at emanuel@texmex.mit.edu.

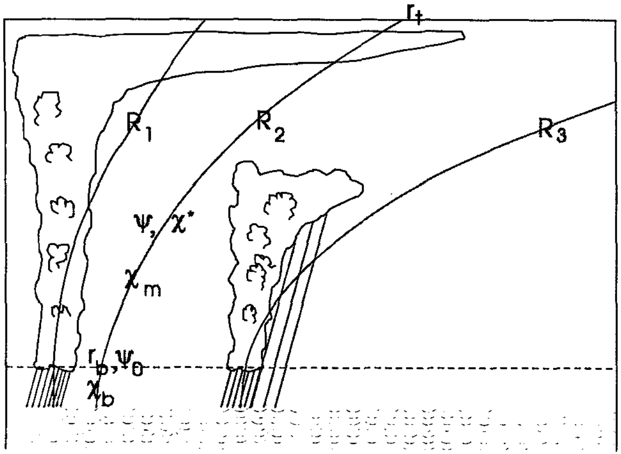

FIG. 1. Structure of the model. Potential radius, R, is used as the model radial coordinate; r_b is the physical radius of R surfaces at the sea surface; and r_t is the physical radius of R surfaces at the tropopause. These are predicted quantities. The thermodynamic variables are χ_b, χ^*, and χ_m, and the mass streamfunction ψ is defined in the midtroposphere. Term ψ_0 is the diagnosed streamfunction at the top of the subcloud layer.

The model is axisymmetric and phrased in angular momentum coordinates, using the potential radius R, defined such that

$$\frac{f}{2}R^2 \equiv rV + \frac{f}{2}r^2. \tag{14}$$

Here f is the Coriolis parameter (assumed constant), r the (physical) radius from the storm center, and V the azimuthal velocity. The right side of (14) is the total angular momentum per unit mass.

The model consists of two parts: a subcloud layer and the rest of the troposphere (see Fig. 1). The latter is assumed always to be in hydrostatic and gradient wind balance and to be neutral to *slantwise* moist convection, a condition approximated by constant s^* along angular momentum (R) surfaces. The primary dynamic variables of the model are

- r_b the radius of R surfaces at the sea surface;
- r_t the radius of R surfaces at the tropopause;
- ψ the mean mass streamfunction in the midtroposphere;[3]
- ψ_0 the mass streamfunction at the top of the boundary layer;[3]
- M_u the convective updraft mass flux at the boundary-layer top;
- M_d the convective downdraft mass flux at the boundary-layer top.

[3] In E89, ψ and ψ_0 were defined in terms of the airflow between convective clouds; here they represent the total mass streamfunctions.

All the entropy variables are replaced by a new quantity, χ, defined by

$$\chi \equiv (T_s - T_t)(s - s_{bi}), \tag{15}$$

where T_s and T_t are the surface and tropopause absolute temperatures (assumed constant), s is the entropy, and s_{bi} is the entropy of the ambient subcloud layer. Thus, the subcloud-layer entropy variable used in the model is χ_b, the troposphere entropy variable is χ_m, and the saturation entropy of the troposphere is χ^*:

$$\chi_b \equiv (T_s - T_t)(s_b - s_{bi}),$$
$$\chi_m \equiv (T_s - T_t)(s_m - s_{bi}),$$
$$\chi^* \equiv (T_s - T_t)(s^* - s_{bi}). \tag{16}$$

Clearly, $\chi_b = \chi^* = 0$ in the ambient environment (which is assumed to be convectively neutral) and $\chi_m \leq 0$.

All the entropy variables, χ, are scaled in the model by the ambient value of χ at saturation at sea surface temperature:

$$\chi_s \equiv (T_s - T_t)(s^*_{si} - s_{bi}), \tag{17}$$

where s^*_{si} is the ambient saturation entropy of the ocean surface. (Here s^*_s varies with radius because of the dependence of s^* on pressure.) The quantity χ_s has the units of velocity squared, with typical values around 3600 $m^2\,s^{-2}$. E89 showed that a characteristic maximum surface wind speed in tropical cyclones is $\overline{\chi}_s^{1/2}$, of order 60 m s^{-1}.

All the dependent and independent variables are made dimensionless according to the scaling in Table 1, which also shows typical numerical values of the scaling parameters, and the definitions and values of the nondimensional model parameters are given in Table 2.

TABLE 1. Scaling parameters.

Variable	Scaled by[a]	Typical value[b]
Dependent:		
χ_b, χ_m, χ^*	χ_s	3600 $m^2\,s^{-2}$
r_b, r_t	$\sqrt{\chi_s}/f$	1000 km
V	$\sqrt{\chi_s}$	60 m s^{-1}
ψ, ψ_0	$\frac{1}{2}c_{D0}\rho_s g \chi_s^{3/2} f^{-2}$	4×10^{11} kg m s^{-3}
w_e, w_m, M_u, M_d	$c_{D0}\sqrt{\chi_s}$	6 cm s^{-1}
$\ln(p/p_0)$	$\chi_s/R_d T_s$	0.04
Independent:		
R	$\sqrt{\chi_s}/f$	1000 km
τ	$c_{D0}^{-1}\frac{R_d T_s}{g}\frac{\Delta P}{P_0}\chi_s^{-1/2}$	15 hours

[a] See E89 for definitions of the parameters that appear here.
[b] Assuming $T_s = 27°C$, $T_t = -70°C$, $\mathscr{H} = 80\%$, $f = 5 \times 10^{-5}\,s^{-1}$, $p_0 = 1000$ mb, $\Delta P = 400$ mb, $c_{D0} = 10^{-3}$.

The fundamental change from E89 consists of replacing the buoyancy closure for convection used there with the subcloud-layer equilibrium scheme described here in section 1. That is, we use, with some modification, (6), (10), (11), and (12) phrased in potential radius coordinates and scaled according to Table 1. In addition, the scaled form of the subcloud-layer entropy equation, (1), is actually solved, but subject to the constraint (13), which takes the form

$$\chi_b \leqslant \chi^*.$$

One important modification of the new closure is necessary in applying it to the hurricane problem. This consists of taking into account radial entropy advection in the subcloud layer. Accordingly, the dimensionless version of (1) contains a radial advection term, and consequently so does the equilibrium mass flux, whose dimensionless form is given in the appendix by (A9). In other words, the equilibrium downdraft mass flux into the subcloud layer is assumed to balance surface fluxes *and* radial entropy advection by the Ekman flow.

There are two further critical aspects of the new closure that must be addressed. First, E89 showed that the quintessential physical process leading to tropical cyclone genesis in the model is the cessation of convective downdrafts owing to saturation of the middle and lower troposphere on the mesoscale. Thus, unlike in the linear analyses of tropical intraseasonal oscillations (Emanuel 1993), we must here allow for a variable bulk precipitation efficiency ϵ_p. Qualitatively, one would expect ϵ_p to vary with the relative humidity of the lower and middle troposphere. Accordingly, we choose the function

$$\epsilon_p = \frac{\chi_m - \chi_{m0}}{\chi_b - \chi_{m0}}, \qquad (18)$$

where χ_{m0} is the initial entropy deficit of the midtroposphere. Thus, ϵ_p is zero in the environment and approaches unity as $\chi_b \rightarrow \chi_m$. At first, this may appear to be an extreme variation of ϵ_p, but it should be noted that we are also applying a Newtonian cooling in place of real radiative cooling. As this cooling vanishes in the environment of the storm, so too must the convective heating for a balance to be maintained.

The second critical process is the moistening of the lower and midtroposphere by convection, since this is the essential process that saturates the troposphere in the incipient cyclone core and allows downdraft-free convection to develop there. The effect of convection on free-atmosphere entropy can be broken into two parts: entropy advection by subsiding air in the cloud environment, and detrainment of high entropy, cloudy air. As we shall see, the development of tropical cyclones in the model is sensitive to the distribution and magnitude of moistening of the lower troposphere by convection. In the present model, the detrainment of entropy into the lower troposphere is formulated as

$$M_u(\chi_b - \chi_m)[\Lambda_{\max}(1 - \epsilon_p) + \Lambda_{\min}\epsilon_p], \qquad (19)$$

where $\Lambda_{\max}$ and $\Lambda_{\min}$ are parameters that govern the rate of detrainment of high-entropy, cloudy air into the lower troposphere. Both $\Lambda_{\max}$ and $\Lambda_{\min}$ are less than unity, and it is assumed that that portion of the entropy detrainment that does not occur in the lower troposphere takes place in the upper troposphere so as to satisfy integral entropy conservation. When $\epsilon_p = 0$, it is assumed that a greater fraction of detrainment occurs in the lower troposphere, while when ϵ_p is close to unity, most of the detrainment happens in the upper troposphere. Note that the entropy of the upper troposphere is not a model variable.

Aside from the representation of convection, the model differs from that of E89 in the following respects.

1) Momentum diffusion has been added to the top layer. This has the cosmetic effect of preventing real discontinuities from forming at the model top but is observed to have little effect otherwise.

2) The enthalpy surface exchange coefficient is allowed to differ from the surface drag coefficient.

3) The magnitude of the radiative cooling, while still capped, is not turned off in regions of positive Ekman pumping as in E89.

4) The other variables, χ_m^* and ω_d, used in E89 are not needed here.

5) There is no downward advection of entropy from the upper to the lower troposphere.

Most of these differences are minor in comparison to the implementation of the new representation of convection and have the effect of simplifying the model.

3. Results

Figure 2 shows the evolution with time of the maximum azimuthal velocity in a control run and compares it with the result of running the original model of E89. Both have been initialized using the warm-core vortex and boundary conditions described in E89, with parameter values listed in Table 2. The evolutions, as well as the radial distributions of variables (not shown), are very similar in the two cases. Given that the only substantive difference here is the use of a cumulus scheme based on subcloud-layer equilibrium, the similarity of the results of running both models supports the conclusion of E89 that the hurricane subcloud layer is very nearly in equilibrium, even during rapid development.

In other respects, as well, the reformulated model behaves very similarly to the original, displaying the same sensitivity to the control parameters and initial conditions. The sensitivity to the convective relaxation timescale τ_c, which appears in (A10), is weak. On the other hand, the model proves very sensitive to the pa-

TABLE 2. Nondimensional model parameters.

Parameter	Name	Definition[a]	Value used in control experiment
Control parameters:			
Q	Static stability	$\frac{\Gamma_d}{\Gamma_m} c_p(T_s - T_t)\chi_s^{-1}\Delta P \left(-\frac{\partial \ln\theta}{\partial p}\right)$	2
$\frac{T_s - T_t}{T_s}$	Thermodynamic efficiency	—	1/3
$\mathcal{H}$	Ambient surface relative humidity	—	0.8
$\frac{C_k}{C_D}$	Ratio of exchange coefficients	—	1.0
β	Isothermal expansion parameter	$\frac{\chi_s}{R_d T_s}$	0.042
τ_c	Convective timescale	$c_{D0}\frac{g}{R_d T_s}\frac{p_0}{\Delta P}\chi_s^{1/2}\tau_c$	0.05
l	Eddy mixing scale	$l_d f^{3/2}\chi_s^{-3/4}c_{D0}^{-1/2}\left(\frac{R_d T_s}{g}\frac{\Delta P}{p_0}\right)^{1/2}$	$0.03\Delta R$
b	Radiative relaxation rate	$c_{D0}^{-1}\frac{R_d T_s}{g}\frac{\Delta P}{p_0}\chi_s^{-1/2}\tau_{rad}^{-1}$	2
c	Wind dependence of surface fluxes	$c_{D1}c_{D0}^{-1}\chi_s^{1/2}$	2
Λ_{max}	Maximum entropy detrainment coefficient	—	0.6
Λ_{min}	Minimum entropy detrainment coefficient	—	0.3
γ	Boundary-layer relative depth	$\Delta P_b \Delta P^{-1}$	0.1
Initial conditions:			
r_m	Radius of maximum winds	—	0.05
r_0	Radius of vanishing wind	—	0.35
V_m	Maximum azimuthal wind	—	0.3
χ_{m0}	Lower-tropospheric entropy deficit	—	−1.0
Numerical parameters:			
NR	Number of nodes (including boundaries)	—	30
$\Delta\tau$	Time step	—	0.001
R_0	Radius of outer wall	—	1.0

[a] See E89 for definitions of parameters.

rameters Λ_{max} and Λ_{min} that are present in the lower-tropospheric entropy equation, (A8), as illustrated in Fig. 3. This is hardly surprising in view of the arguments set forth in section 2.

As suggested by E89, *the near saturation of a mesoscale column of the troposphere at the cyclone core is a necessary condition for intensification.* This conjecture is also supported by the results of a recent field experiment (Emanuel 1994b). Only when the troposphere is nearly saturated are the downdrafts that normally accompany deep convection suppressed; this allows surface fluxes to actually increase the entropy of the subcloud layer and, through moist adiabatic adjustment, the temperature of the troposphere. This conclusion is also supported by an experiment in which the initial vortex is very weak but a mesoscale column is saturated initially. As shown in Fig. 4, the small initial disturbance grows rapidly, whereas the same disturbance in the normal tropical atmosphere, with low θ_e aloft everywhere, dies.

One interesting aspect of the model's behavior is the appearance of multiple eyewalls when the initial relative humidity of the troposphere is high. Figure 5 shows the updraft mass flux as a function of radius at a particular time for an experiment in which $\chi_{m0} = -0.25$ (compared to -1.0 in the control case). Outer eyewalls form and gradually move inward, while the inner eyewalls dissipate, resembling the observed behavior of concentric eyewall cycles (Willoughby et al. 1982). The mean position of the eyewall as well as the entire storm circulation expand very gradually in the radial direction during these model cycles.

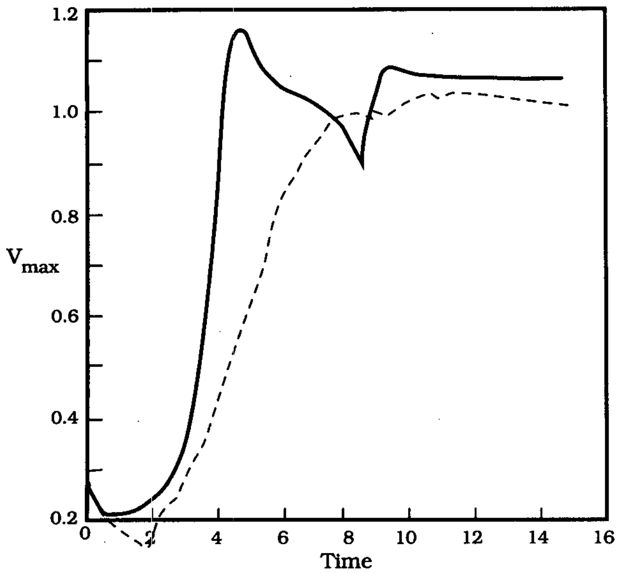

FIG. 2. Evolution with (nondimensional) time of the maximum (nondimensional) azimuthal velocity for the control run of the present model (solid) and of the original E89 model (dashed) run with the same parameters and initial and boundary conditions.

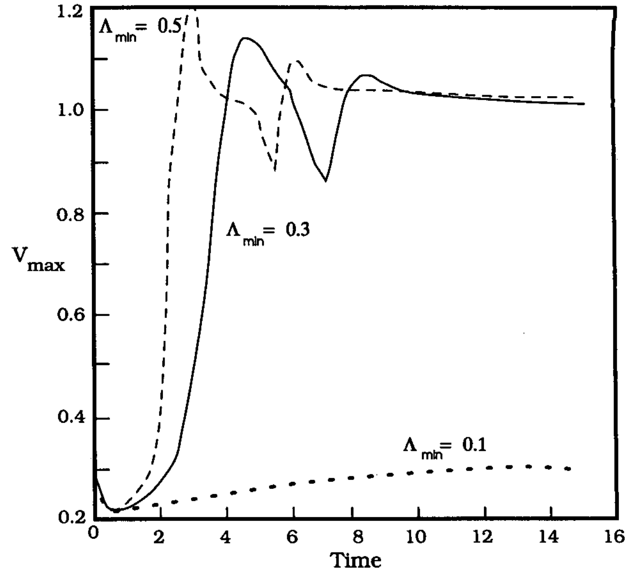

FIG. 3. Evolution with time of the maximum azimuthal velocity for three different values of the parameter Λ_{min}, which influences the rate of moistening of the lower troposphere by convection.

4. Summary

Scaling analysis and experience with numerical models (e.g., E89) strongly suggest that subcloud layers are nearly in thermodynamic equilibrium, with heat fluxes from the surface nearly balancing convective and small-scale turbulent fluxes of entropy through the subcloud-layer top. Assuming such a balance leads to a restraint (4) on equilibrium convective updraft mass flux, which shows that it is proportional to the surface enthalpy flux and the large-scale ascent rate just above the subcloud layer. A closed convective representation also requires a relationship between downdraft and updraft mass fluxes and a link between tendencies of temperature in the lower and upper troposphere; both of these require a cloud model. (A cloud model is also required to predict the moistening of the free-troposphere by convection.) But for the purposes of a simple model, we assume that the convective updraft and downdraft mass fluxes are proportional, with the proportionality related to a (variable) bulk precipitation efficiency, as in (6). The specification of both the convective updraft and downdraft mass fluxes allows for the prediction of lower-tropospheric saturation entropy (i.e., temperature), and the subcloud-layer entropy is *diagnosed* by assuming that it is equal to the lower-tropospheric saturation entropy in regions of convection.

Use of such a subcloud equilibrium-based convection scheme was shown by Emanuel (1993) to yield realistic phase speeds and amplification rates of large-scale equatorial disturbances, provided small lags in the convective mass flux response were used. Here we have shown that this type of convection scheme also works very well in a simple model of tropical cyclones, with an expected sensitivity to the dependence of the bulk precipitation efficiency on environmental parameters such as relative humidity. These results support the

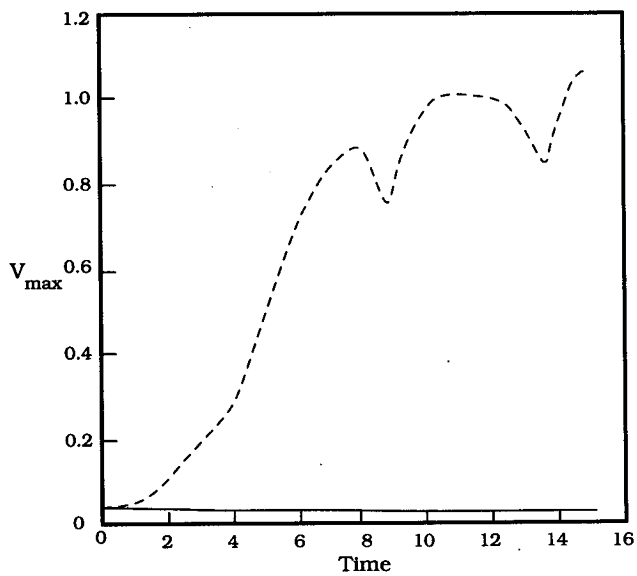

FIG. 4. Evolution with time of the maximum azimuthal velocity for a run identical to the control but starting with a velocity amplitude of only 0.05 (solid), and a similar run but starting from a condition in which the whole atmospheric column is saturated inside the radius $R = 0.15$ (dashed).

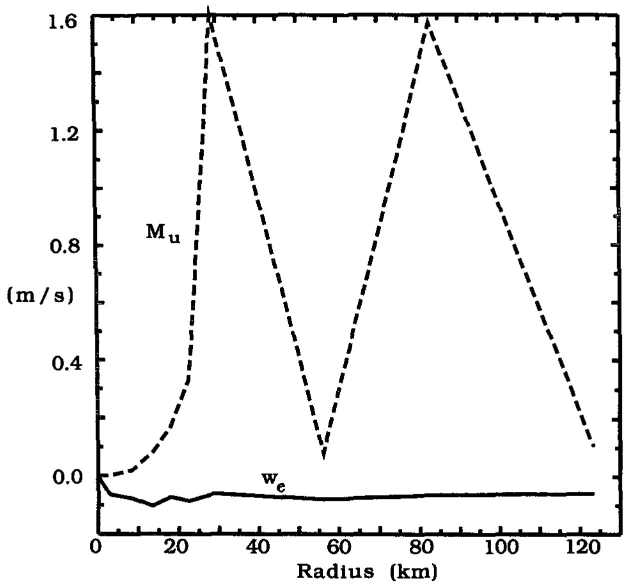

FIG. 5. The convective updraft volume flux (M_u) and clear-air vertical velocity (w_e) at 6.8 days, plotted as a function of radius from the storm center, in a run identical to the control but with the initial entropy deficit of the midtroposphere, χ_{m0} reduced to -0.25. For perspective, the radius and velocity scales have been expressed in dimensional terms using the typical scaling values shown in Table 1. A new eyewall has just formed near 80-km radius; it then moved slowly inward while the inner eyewall dissipated.

conclusion of Raymond (1995) that thermodynamic quasi equilibrium of the subcloud layer may provide an important and useful closure condition in the representation of the ensemble effects of cumulus convection.

Acknowledgments. This research was supported by the National Science Foundation under Grant ATM-9216906. The author thanks Alan Betts, David Raymond, and an anonymous reviewer for their helpful remarks.

APPENDIX

Summary of Model Equations

The equations governing the model dynamics are the same as those of E89 except for the changes noted in section 2. The nondimensional model equations are summarized as follows, with the scaling of the dependent and independent variables given in Table 1. Typical values of the scaling parameters are also shown in Table 1, and the definitions of all the nondimensional parameters are given in Table 2.

Thermal wind:

$$\frac{1}{r_b^2} = \frac{1}{r_t^2} - \frac{2}{R^3}\frac{d\chi^*}{dR}. \quad \text{(A1)}$$

Mass:

$$\frac{\partial r_b^2}{\partial \tau} = \psi_0 - \psi + D_b, \quad \text{(A2)}$$

$$\frac{\partial r_t^2}{\partial \tau} = \psi + D_t \quad \text{(see fn 4)}. \quad \text{(A3)}$$

Streamfunction at boundary-layer top:

$$\psi_0 = (1 + c|V_b|)|V_b| \frac{1}{2R}\frac{\partial r_b^2}{\partial R}(R^2 - r_b^2). \quad \text{(A4)}$$

Saturation entropy at boundary-layer top:

$$\frac{\partial \chi^*}{\partial \tau} = Q\left(M_u + M_d - \frac{\partial \psi}{\partial r_i^2}\right) + D_{\chi^*} - \text{rad}. \quad \text{(A5)}$$

The model equation for the subcloud-layer entropy is (1), subject to the condition (13), transformed into potential radius coordinates, and nondimensionalized according to Table 1.

Subcloud-layer entropy:

$$\gamma \frac{\partial \chi_b}{\partial \tau} = \psi_0 \frac{\partial \chi_b}{\partial r_b^2} - \frac{1}{2}(|w_e| - w_e + |M_d| - M_d)(\chi - \chi_m) + \frac{C_k}{C_D}(1 + c|V_b|)|V_b|(\chi_s^* - \chi_b), \quad \text{(A6)}$$

subject to the constraint

$$\chi_b \leq \chi^*. \quad \text{(A7)}$$

Lower-tropospheric entropy:

$$\frac{\partial \chi_m}{\partial \tau} = -\frac{1}{2}(|w_e| + w_e)(\chi_b - \chi_m) + M_u(\chi_b - \chi_m)[\Lambda_{\max}(1 - \epsilon_p) + \Lambda_{\min}\epsilon_p] - \frac{\Gamma_m}{\Gamma_d}\text{rad}. \quad \text{(A8)}$$

The convective mass fluxes are given by nondimensional forms of (4), (6), and (11), transformed into potential radius coordinates and nondimensionalized according to Table 1. Note, however, that owing to the highly baroclinic nature of the hurricane eyewall, we must include horizontal entropy advection in the entropy balance:

$$M_{u_{eq}} = \frac{\partial \psi_0}{\partial r_b^2} + \frac{\psi_0 \frac{\partial \chi_b}{\partial r_b^2} + (1 + c|V_b|)|V_b|(\chi_s^* - \chi_b)}{\chi_b - \chi_m}, \quad \text{(A9)}$$

[4] The term D_t was omitted in E89; see section 2.

$$\frac{\partial M_u}{\partial \tau} = \psi_0 \frac{\partial M_u}{\partial r_b^2} + \frac{(M_{u_{eq}} - M_u)}{\tau_c}, \qquad \text{(A10)}$$

$$M_d = -(1 - \epsilon_p)M_u. \qquad \text{(A11)}$$

There are, in addition, the following diagnostic relations.

Azimuthal velocity:

$$V_b = \frac{1}{2}\frac{R^2 - r_b^2}{r_b}. \qquad \text{(A12)}$$

Momentum diffusion in boundary layer:

$$D_b = -\frac{1}{R}\frac{\partial}{\partial R}\left[r_b^2 \nu_b \frac{\partial}{\partial r_b}\left(\frac{R^2}{r_b^2}\right)\right]. \qquad \text{(A13)}$$

Momentum diffusion, top layer:

$$D_t = -\frac{1}{R}\frac{\partial}{\partial R}\left[r_t^2 \nu_t \frac{\partial}{\partial r_t}\left(\frac{R^2}{r_t^2}\right)\right]. \qquad \text{(A14)}$$

Eddy viscosities:

$$\nu_b = l^2 \left| r_b \frac{\partial}{\partial r_b}\left(\frac{R^2}{r_b^2}\right)\right|,$$

$$\nu_t = l^2 \left| r_t \frac{\partial}{\partial r_t}\left(\frac{R^2}{r_t^2}\right)\right|. \qquad \text{(A15)}$$

Heat diffusion:

$$D_\chi = \frac{\partial}{\partial r_b^2}\left(r_b \nu_b \frac{\partial \chi^*}{\partial r_b}\right). \qquad \text{(A16)}$$

Radiation:

$$\text{rad} = -b\chi^*, \qquad \text{(A17)}$$

subject to

$$\text{rad} \leq \text{rad}_c.$$

Saturation entropy of sea surface:

$$\chi_s^* = 1 - \frac{T_s - T_t}{T_s} P + \frac{1}{1 - \mathcal{H}}(e^{-\beta P} - 1). \qquad \text{(A18)}$$

Surface pressure (cyclostrophic relation):

$$\frac{\partial}{\partial R}\left[P + \chi^* + \frac{1}{8}\left(\frac{R^4}{r_b^2} + r_b^2\right)\right] = \frac{1}{2}\frac{R^3}{r_t^2}. \qquad \text{(A19)}$$

Clear air vertical velocity at boundary-layer top:

$$w_e = \frac{\partial \psi_0}{\partial r_b^2} - M_u - M_d. \qquad \text{(A20)}$$

Bulk precipitation efficiency:

$$\epsilon_p = \frac{\chi_m - \chi_{m0}}{\chi_b - \chi_{m0}}. \qquad \text{(A21)}$$

Radius of R surfaces in midtroposphere:

$$\frac{1}{r_i^2} = \frac{1}{2}\left(\frac{1}{r_b^2} + \frac{1}{r_t^2}\right). \qquad \text{(A22)}$$

The model consists of (A1)–(A22) with nondimensional parameters described in Table 2.

REFERENCES

Arakawa, A., and W. H. Schubert, 1974: Interaction of a cumulus cloud ensemble with the large-scale environment. Part I. *J. Atmos. Sci.,* **31,** 674–701.

Betts, A. K., 1986: A new convective adjustment scheme. Part I: Observational and theoretical basis. *Quart. J. Roy. Meteor. Soc.,* **112,** 677–691.

——, and M. J. Miller, 1986: A new convective adjustment scheme. Part II: Single column tests using GATE wave, BOMEX, ATEX and arctic air-mass data sets. *Quart. J. Roy. Meteor. Soc.,* **112,** 693–709.

Bretherton, C. S., and P. K. Smolarkiewicz, 1989: Gravity waves, compensating subsidence, and detrainment around cumulus clouds. *J. Atmos. Sci.,* **46,** 740–759.

Emanuel, K. A., 1989: The finite-amplitude nature of tropical cyclogenesis. *J. Atmos. Sci.,* **46,** 3431–3456.

——, 1993: The effect of convective response time on WISHE modes. *J. Atmos. Sci.,* **50,** 1763–1775.

——, 1994a: *Atmospheric Convection.* Oxford University Press, 580 pp.

——, 1994b: The physics of tropical cyclogenesis over the eastern Pacific. *Tropical Cyclone Disasters,* J. Lighthill, Z. Zhemin, G. Holland, and K. Emanuel, Eds., Peking University Press, 588 pp.

——, J. D. Neelin, and C. S. Bretherton, 1994: On large-scale circulations in convecting atmospheres. *Quart. J. Roy. Meteor. Soc.,* **120,** 1111–1143.

Manabe, S., J. Smagorinsky, and R. F. Strickler, 1965: Simulated climatology of a general circulation model with a hydrologic cycle. *Mon. Wea. Rev.,* **93,** 769–798.

Neelin, J. D., and J. Yu, 1994: Modes of tropical variability under convective adjustment and the Madden–Julian oscillation. Part I: Analytical theory. *J. Atmos. Sci.,* **51,** 1876–1894.

Raymond, D. J., 1995: Regulation of moist convection over the west Pacific warm pool. *J. Atmos. Sci.,* **52,** 3945–3959.

Willoughby, H. E., J. A. Clos, and M. G. Shoreibah, 1982: Concentric eyes, secondary wind maxima, and the evolution of the hurricane vortex. *J. Atmos. Sci.,* **39,** 395–411.

Yano, J.-I., and K. A. Emanuel, 1991: An improved model of the equatorial troposphere and its coupling with the atmosphere. *J. Atmos. Sci.,* **48,** 377–389.